Pressure-Driven Orbital Selective Insulator to Metal Transition and Spin State Crossover in Cubic CoO

Li Huang,[1,2] Yilin Wang,[1] and Xi Dai[1]

[1] *Beijing National Laboratory for Condensed Matter Physics, and Institute of Physics, Chinese Academy of Sciences, Beijing 100190, China*

[2] *National Key Laboratory for Surface Physics and Chemistry, P.O. Box 718-35, Mianyang 621907, Sichuan, China*

(Dated: December 14, 2011)

The metal-insulator and spin state transitions of CoO under high pressure are studied by using density functional theory combined with dynamical mean-field theory. Our calculations predict that the metal-insulator transition in CoO is a typical orbital selective Mott transition, where the t_{2g} orbitals of Co $3d$ shell become metallic firstly around 60 GPa while the e_g orbitals still remain insulating until 170 GPa. Further studies of the spin states of Co $3d$ shell reveal that the orbital selective Mott phase in the intermediate pressure regime is mainly stabilized by the high-spin state of the Co $3d$ shell and the transition from this phase to the full metallic state is driven by the high-spin to low-spin transition of the Co^{2+} ions. Our results are in good agreement with the most recent transport and x-ray emission experiments under high pressure.

PACS numbers: 71.30.+h, 71.27.+a, 75.30.Wx, 91.60.Gf

Although the Mott metal-insulator transition (MIT) has been studied extensively for decades, most of the works are focused on the single band Hubbard model, where the Mott transition is driven completely by the ratio of the local Coulomb interaction and band width. While most of the Mott MITs in realistic materials[1] involve more than one band where the transition is driven not only by the local Coulomb interaction but also by the distribution of the electrons among these bands. For example, the redistribution of the four electrons among three bands may lead to so-called orbital selective Mott transition (OSMT)[2–7] in the t_{2g} bands. On the other hand, in many systems the redistribution of the electrons among different bands is induced by the crossover in spin states, i.e. the high-spin (HS) to low-spin (LS) transition[8]. Therefore in realistic materials (e.g. in $3d$ transition metal compounds) the Mott MIT and spin state crossovers are closely related to each other[9–15].

Recently the high pressure experiments on charge transfer insulator CoO revealed very interesting behaviors in both transport properties and x-ray emission spectroscopy (XES). The transport measurement[16] indicated that with the increment of pressure there are two transitions in resistivity, one happens around 60 GPa and the other one takes place around 130 GPa. While the room temperature XES measurements[17, 18] on the similar sample show that the spin state of Co^{2+} ions persist in the HS state all the way to 140 GPa, after which the crossover from HS to LS states happens. Hence the interplay between the HS-LS transition and the two-step Mott insulator transition becomes the key factor to understand the underlying physics in CoO.

The pressure-driven MIT and magnetic moment collapse in transition metal oxides have been studied by first principles calculations widely[9–11, 13, 19, 20]. As to CoO, its magnetic state transition under pressure was first discussed[13] within the Stoner scenario by employing the local spin density approximation (LSDA) and generalized gradient approximation (GGA) approaches of density functional theory. A transition from HS to nonmagnetic metallic state was found around 88 GPa. Since these calculations did not take the correlation effects of the Co $3d$ shell into considerations, so the experimentally observed excitation gap for CoO[18] as large as $2.5 \sim 2.6$ eV was not reproduced completely. Recently, Zhang et al.[21] reinvestigated the pressure-driven magnetic phase transition in CoO by using LSDA + U approach. The HS-LS transition is indeed obtained to be of $t_{2g}^5 e_g^2 \rightarrow t_{2g}^6 e_g^1$ character, but the electronic structure transition is insulator to insulator scheme. This contradicts with the resistivity data under high pressure[16], which shows dramatic change in resistivity indicating the insulator to metal transition with pressure.

In this letter, based on the local density approximation (LDA) combined with dynamical mean-field theory (DMFT)[22, 23], we have carried out theoretical calculations for cubic phase CoO at different volumes for the first time. Our calculations show that CoO under pressure is a typical system which has OSMT. At ambient pressure our calculation gives correct Mott insulator phase for CoO with energy gap being around 2.4 eV. At the first transition around 60 GPa the t_{2g} bands become metallic while the e_g bands still remains insulating until the pressure reaches 170 GPa. Therefore in CoO the exotic orbital selective Mott phase (OSMP) with metallic t_{2g} and insulating e_g bands is stable in a quite large pressure window between 60 and 170 GPa. Our LDA+DMFT calculations also find that the Co^{2+} ions remain in HS state during the first transition and the crossover to the LS state starts only after the second transition, which is in good agree-

ment with both the resistivity[16] and XES data [17, 18] in CoO.

The LDA+DMFT calculations[24–26] in the present paper have been carried out by using the pseudopotential plane-wave method with the QUANTUM ESPRESSO package[27] for the LDA part and continuous-time quantum Monte Carlo (CTQMC)[28, 29] as the impurity solver for the DMFT part. The single particle LDA Hamiltonian is obtained by applying a projection onto atomic-centered symmetry-constrained Wannier function (WF) orbitals including all the Co $3d$ and oxygen $2p$ orbitals, which is described in details in Ref.24. That would correspond to a 8×8 $p-d$ Hamiltonian which is a minimal model required for a correct description of the electronic structure of CoO due to its charge transfer nature[1].

The LDA+DMFT calculations presented below have been done for crystal volumes corresponding to values of pressure up to 280 GPa. For simplicity, all first principles calculations were performed in nonmagnetic configuration for rocksalt-type crystal structure with lattice constant scaled to give a volume corresponding to applied pressure. The Coulomb interaction is taken into considerations merely among Co $3d$ orbitals. In the present work, we choose $U = 8.0$ and $J = 0.9$ eV, which are close to previous estimations[21, 30]. We adopt the scheme proposed in reference 11 to deal with the double counting energy. The effective impurity problem for the DMFT was solved by the CTQMC quantum impurity solver (hybridization expansion version) supplemented with recently developed orthogonal polynomial representation algorithm[31]. The maximum entropy method[32] was used to perform analytical continuation to obtain the impurity spectral function of Co $3d$ states. Calculations for all crystal volumes were preformed in paramagnetic state at the temperature of 290 K.

In Fig.1, the evolution of single particle spectrum for Co $3d$ states upon compression is shown. The momentum integrated spectral function $A(\omega)$ under ambient pressure shows well defined insulating behavior for all $3d$ orbitals. However the energy gap for e_g orbitals is slightly higher than that for t_{2g} states indicating that the latter orbitals are closer to MIT than the former ones. At zero pressure, the calculated gap for t_{2g} orbitals of about 2.1 eV and for e_g orbitals of about 2.3 eV, which agree well with optical experimental value 2.6 eV[18]. The LDA+DMFT calculations made for small volume values corresponding to high pressures gave metallic state for CoO starting from 60 GPa in agreement with room temperature resistivity data[16]. One can see that t_{2g} orbitals become metallic whereas e_g ones still remain insulating. This behavior reminds the OSMT scenario as discovered in ruthenates[2] at first. The spectral functions for t_{2g} orbitals in Fig.1 for pressure values larger than 60 GPa become typical for strongly correlated metal close to MIT: well pronounced Hubbard bands and narrow quasiparticle peek. However, the $A(\omega)$ for e_g bands remains insulating with Hubbard

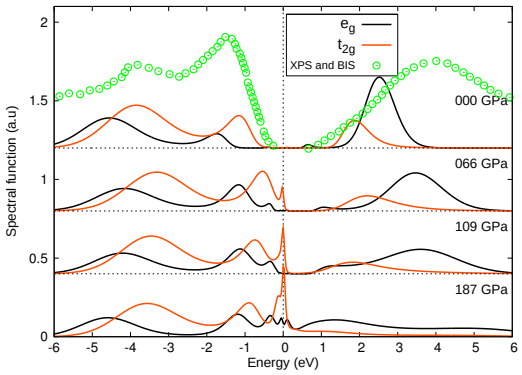

FIG. 1. (Color online) Single particle spectral function of Co $3d$ states vs pressure obtained in LDA+DMFT calculations at room temperature. The spectral function is obtained from imaginary-time green's function $G(\tau)$ by using maximum entropy method[32], and the results are cross-checked by using recently developed stochastic analytical continuation method[33]. The available x-ray photoelectron spectroscopy (XPS) and bremsstrahlung isochromat spectroscopy (BIS) experimental data[18] are drawn in this figure as a comparison.

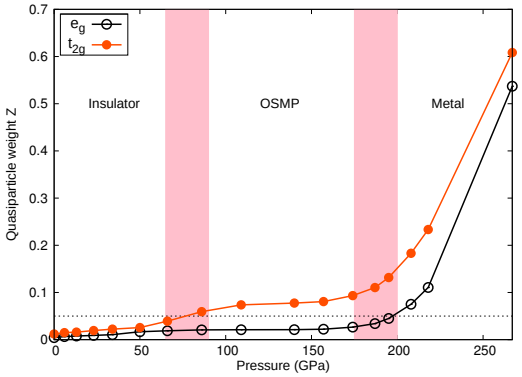

FIG. 2. (Color online) Quasiparticle weight Z of Co $3d$ states as a funtion of pressure. The transition zones are highlighted by pink vertical bars.

bands only but the gap size is strongly reduced comparing with that of ambient pressure. When the pressure exceeds about 170 GPa, the e_g states undergo a insulator to metal transition. As is seen in Fig.1, at 187 GPa the Mott gaps for both $3d$ orbitals disappear finally.

In order to reveal the nature of OSMT in Co $3d$ orbitals upon compression, we make further estimation for their quasiparticle weights by using the well-known equation[22]: $Z^{-1} = 1 - \frac{\partial}{\partial\omega}\mathrm{Re}\Sigma(i\omega)|_{\omega=0}$, where $\mathrm{Re}\Sigma(i\omega)$ is the real part of impurity self-energy function at real frequency axis. In Fig.2 the calculated quasiparticle weights for t_{2g} and e_g states as a function of pressure are shown. It is apparent that the phase diagram can be splitted into three different zones: (1) 0 GPa $<$ P $<$ 60 GPa. The quasiparticle weights for both the e_g and t_{2g} orbitals approach zero, and the system exhibits insulating behavior. (2) 60 GPa $<$ P $<$ 170 GPa. The quasiparticle weights

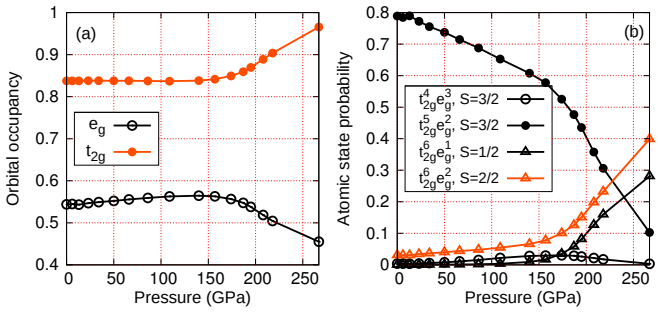

FIG. 3. (Color online)(a) The orbital occupancy of Co 3d states as a function of external pressure. (b) The principal pressure-dependent atomic state probability of Co 3d states obtained by LDA+DMFT calculations.

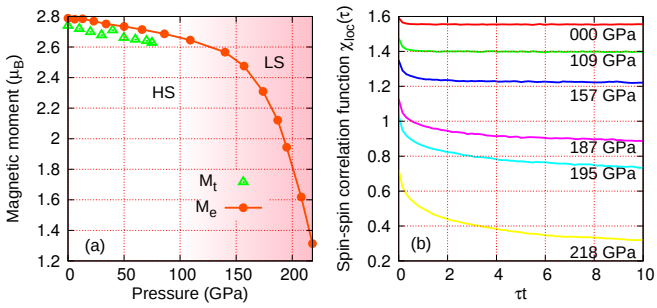

FIG. 4. (Color online) Spin state transition in CoO. (a) Evolution of the local spin magnetic moment of Co 3d states. Here M_e means effective local moment which can be calculated by $\sqrt{T\chi_{loc}}$, and M_t (illustrated by triangle) denotes the previous theoretical results[20]. (b) Spin-spin correlation function $\chi_{loc}(\tau) = \langle S_z(0)S_z(\tau)\rangle$ under various external pressures.

for t_{2g} states become considerable, whereas those for e_g states remain very tiny. At this range of pressure, it gives an exotic OSMP. (3) P $>$ 170 GPa. The quasiparticle weights for both t_{2g} and e_g states show a dramatic increment with pressure, and the system goes into the fully metallic state.

In Fig.3(a) we show the evolution of Co 3d occupancies and the atomic state probability under compression. Due to the charge transfer from O 2p orbitals to Co 3d orbitals, the total 3d states occupation number is ~ 7.2, which is slightly larger than the nominal value 7.0. At ambient pressure, the occupation numbers for t_{2g} and e_g orbitals are $n(e_g) = 0.54$ and $n(t_{2g}) = 0.84$, respectively. Those numbers agree very well with the HS state of Co^{2+} ion in cubic crystal field with two electrons in e_g states and five electrons in t_{2g} states. Over the pressure range from 0 to 170 GPa, the occupation numbers for 3d orbitals basically remains unchanged. While when the pressure is larger than 170 GPa, the occupation numbers for t_{2g} and e_g states show a dramatic change. The $n(t_{2g})$ increases to 1.0 and $n(e_g)$ decreases to 0.25 eventually, which agree well with the LS configuration of Co^{2+} ion ($t_{2g}^6 e_g^1$ character). Thus the evolution of Co 3d occupancies with respect to external pressure provides an strong evidence for the HS-LS spin state crossover in CoO.

During the Monte Carlo simulation, we keep track of the different atomic state configurations visited and draw them as histograms, which give complementary information to the variations of occupancies and magnetic states. In Fig.3(b), we show the histograms for several uppermost $N = 7$ and $N = 8$ atomic state configurations. It is apparent that at ambient pressure, the HS state ($t_{2g}^5 e_g^2$, $S = 3/2$) makes predominant contribution and the contribution from LS state ($t_{2g}^6 e_g^1$, $S = 1/2$) and intermediate spin (IS) state ($t_{2g}^6 e_g^2$, $S = 1$) can be ignored reasonably. As increasing the pressure, the contributions from HS state have dropped and LS state and IS state tend to grow, and the total spin magnetic moment will decrease as well (see Fig.4). We note that except for $t_{2g}^5 e_g^2$ configuration, the contribution from another HS configuration $t_{2g}^4 e_g^3$ ($S = 3/2$) is very little. Thus it is confirmed that the HS-LS spin state transition for CoO has a $t_{2g}^5 e_g^2 \rightarrow t_{2g}^6 e_g^1$ character, which is consistent with previous assumptions[17, 21]. In addition, the contribution to magnetic collapse in CoO from HS-IS spin state transition ($t_{2g}^5 e_g^2 \rightarrow t_{2g}^6 e_g^2$ character) can not be neglected as well.

Next, we concentrate our attentions to the magnetic properties of cubic CoO under pressure. In Fig.4(a) it shows the evolution of the local spin magnetic moment with pressure. We note that the effective local moment M_e is defined through the local spin susceptibility $\sqrt{T\chi_{loc}}$, where χ_{loc} is defined as $\chi_{loc} = \int_0^\beta d\tau \chi_{loc}(\tau) = \int_0^\beta d\tau \langle S_z(0)S_z(\tau)\rangle$. As is clearly seen in Fig.4(a), under compression the local moment decreases slightly from its ambient pressure HS value down to about 170 GPa. Further compression rapidly degrades the moment, which is accompanied by the redistribution of electrons $e_g \rightarrow t_{2g}$ within the Co 3d shell (see Fig.3). It should be pointed out that at low pressure region our results coincide with previously published theoretical results[13, 20].

In Fig.4(b), the spin-spin correlation function $\chi_{loc}(\tau)$ under various external pressure values are illustrated. For high pressure, a Fermi liquid phase (LS state) is identified. While for low pressure, CoO exhibits a well-defined frozen moment phase (HS state). In the Fermi liquid phase, the spin-spin correlation function behaves as $\chi(\tau) \sim (T/\sin(T\tau\pi))^2$ for times τ sufficiently far from $\tau = 0$ or β, respectively. For P $\geq$ 170 GPa, it displays significant Fermi liquid behaviors, which is consistent with the obtained OSMT phase diagram (see Fig.2) for CoO. The frozen moment phase is characterized by a spin-spin correlation function that approaches a non-zero constants at large times, as is seen from 0 to 170 GPa. Thus this figure reveals a phase transition between a LS Fermi liquid metallic phase and a HS Mott phase with frozen moments

again.

Now we discuss the most interesting issue of this paper, the relationship between OSMT and HS-LS transition. The detail analysis of the spin state indicates that the HS-LS transition is the most important driving force for the OSMT in CoO. Once the Co^{2+} ions keep in HS state, the e_g bands are always half filled, which greatly favors Mott insulator phase and very hard to become metallic. On the other hand, in the HS state the filling factor of t_{2g} bands is only 1/6 (in terms of hole density), which makes it much easier to become metallic. For example, the previous studies on multiband Hubbard model[34] show that the critical U_c for half-filled two-bands model is around $1.7W$ and that of the 1/6 filling three-bands model is around $2.1W$, where W is the band width. Thus apparently it is the different situation in filling factors between e_g and t_{2g} bands which makes the two sub-shells behave so differently under pressure. Once the LS state stabilized above 170 GPa, the e_g orbitals are no longer half filling and turn to the metallic phase eventually.

In summary, we conclude that the two-step like Mott transition in CoO can be understood as a typical OSMT. At ambient pressure CoO is a typical Mott insulator with energy gap around 2.4 eV. At the first transition around 60 GPa the t_{2g} bands become metallic while the e_g bands still remains insulating until the pressure reaches 170 GPa. Therefore in CoO the intriguing OSMP with metallic t_{2g} and insulating e_g bands is stable in a quite large pressure window between 60 and 170 GPa. Our theoretical calculations also find that the Co^{2+} ions remain in HS states during the first transition and the crossover to the LS states starts only after the second transition, which is in good agreement with both the resistivity[16] and XES data[17, 18] for CoO. Further analysis of the calculated results show that the HS-LS transition is the main driving force of the Mott MIT in cubic CoO.

We acknowledge financial support from the National Science Foundation of China and that from the 973 program of China under Contract No.2007CB925000 and No. 2011CBA00108. All the LDA+DMFT calculations have been performed on the SHENTENG7000 at Supercomputing Center of Chinese Academy of Sciences (SCCAS).

[1] M. Imada, A. Fujimori, and Y. Tokura, Rev. Mod. Phys. **70**, 1039 (1998).
[2] V. I. Anisimov, I. A. Nekrasov, D. E. Kondakov, T. M. Rice, and M. Sigrist, Eur. Phys. J. B **25**, 191 (2002).
[3] A. Liebsch, Phys. Rev. Lett. **91**, 226401 (2003).
[4] A. Koga, N. Kawakami, T. M. Rice, and M. Sigrist, Phys. Rev. Lett. **92**, 216402 (2004).
[5] A. Koga, N. Kawakami, T. M. Rice, and M. Sigrist, Phys. Rev. B **72**, 045128 (2005).
[6] L. de'Medici, A. Georges, and S. Biermann, Phys. Rev. B **72**, 205124 (2005).
[7] L. de' Medici, S. R. Hassan, M. Capone, and X. Dai, Phys. Rev. Lett. **102**, 126401 (2009).
[8] P. Werner and A. J. Millis, Phys. Rev. Lett. **99**, 126405 (2007).
[9] J. Kuneš, A. V. Lukoyanov, V. I. Anisimov, R. T. Scalettar, and W. E. Pickett, Nat Mater **7**, 198 (2008).
[10] J. Kuneš, D. M. Korotin, M. A. Korotin, V. I. Anisimov, and P. Werner, Phys. Rev. Lett. **102**, 146402 (2009).
[11] A. O. Shorikov, Z. V. Pchelkina, V. I. Anisimov, S. L. Skornyakov, and M. A. Korotin, Phys. Rev. B **82**, 195101 (2010).
[12] I. S. Lyubutin, S. G. Ovchinnikov, A. G. Gavriliuk, and V. V. Struzhkin, Phys. Rev. B **79**, 085125 (2009).
[13] R. E. Cohen, I. I. Mazin, and D. G. Isaak, Science **275**, 654 (1997).
[14] A. G. Gavriliuk, V. V. Struzhkin, I. S. Lyubutin, S. G. Ovchinnikov, M. Y. Hu, and P. Chow, Phys. Rev. B **77**, 155112 (2008).
[15] A. Mattila, J.-P. Rueff, J. Badro, G. Vankó, and A. Shukla, Phys. Rev. Lett. **98**, 196404 (2007).
[16] T. Atou, M. Kawasaki, and S. Nakajima, Jpn. J. Appl. Phys. **43**, L1281 (2004).
[17] J.-P. Rueff, A. Mattila, J. Badro, G. Vank, and A. Shukla, J. Phys.: Condens. Matter **17**, S717 (2005).
[18] E. Z. Kurmaev, R. G. Wilks, A. Moewes, L. D. Finkelstein, S. N. Shamin, and J. Kuneš, Phys. Rev. B **77**, 165127 (2008).
[19] D. Kasinathan, J. Kuneš, K. Koepernik, C. V. Diaconu, R. L. Martin, I. D. Prodan, G. E. Scuseria, N. Spaldin, L. Petit, T. C. Schulthess, and W. E. Pickett, Phys. Rev. B **74**, 195110 (2006).
[20] U. Wdowik and D. Legut, J. Phys. Chem. Sol. **69**, 1698 (2008).
[21] W. Zhang, K. Koepernik, M. Richter, and H. Eschrig, Phys. Rev. B **79**, 155123 (2009).
[22] A. Georges, G. Kotliar, W. Krauth, and M. J. Rozenberg, Rev. Mod. Phys. **68**, 13 (1996).
[23] G. Kotliar, S. Y. Savrasov, K. Haule, V. S. Oudovenko, O. Parcollet, and C. A. Marianetti, Rev. Mod. Phys. **78**, 865 (2006).
[24] D. Korotin, A. Kozhevnikov, S. Skornyakov, I. Leonov, N. Binggeli, V. Anisimov, and G. Trimarchi, Eur. Phys. J. B **65**, 91 (2008).
[25] G. Trimarchi, I. Leonov, N. Binggeli, D. Korotin, and V. I. Anisimov, J. Phys: Condens. Matter **20**, 135227 (2008).
[26] B. Amadon, F. Lechermann, A. Georges, F. Jollet, T. O. Wehling, and A. I. Lichtenstein, Phys. Rev. B **77**, 205112 (2008).
[27] P. Giannozzi, S. Baroni, N. Bonini, M. Calandra, R. Car, C. Cavazzoni, D. Ceresoli, G. L. Chiarotti, M. Cococcioni, I. Dabo, A. Dal Corso, S. de Gironcoli, S. Fabris, G. Fratesi, R. Gebauer, U. Gerstmann, C. Gougoussis, A. Kokalj, M. Lazzeri, L. Martin-Samos, N. Marzari, F. Mauri, R. Mazzarello, S. Paolini, A. Pasquarello, L. Paulatto, C. Sbraccia, S. Scandolo, G. Sclauzero, A. P. Seitsonen, A. Smogunov, P. Umari, and R. M. Wentzcovitch, J. Phys: Condens. Matter **21**, 395502 (2009).
[28] P. Werner, A. Comanac, L. de' Medici, M. Troyer, and A. J. Millis, Phys. Rev. Lett. **97**, 076405 (2006).
[29] E. Gull, A. J. Millis, A. I. Lichtenstein, A. N. Rubtsov, M. Troyer, and P. Werner, Rev. Mod. Phys. **83**, 349 (2011).

[30] V. I. Anisimov, J. Zaanen, and O. K. Andersen, Phys. Rev. B **44**, 943 (1991).
[31] L. Boehnke, H. Hafermann, M. Ferrero, F. Lechermann, and O. Parcollet, Phys. Rev. B **84**, 075145 (2011).
[32] M. Jarrell and J. Gubernatis, Phys. Rep. **269**, 133 (1996).
[33] K. S. D. Beach, arXiv:0403055 [cond-mat].
[34] J. E. Han, M. Jarrell, and D. L. Cox, Phys. Rev. B **58**, R4199 (1998).